Efficacy of Nano Composite Porous 3D Scaffold of Crab Shell and Al-Kharit Histological and Radiological for Bone Repair *in Vivo*

Saad H. Zebon*[1], Mohammed J. Eesa [2] and Bahaa F. Hussein [3]

[1]Ministry of Agriculture, Veterinary Directorate, Veterinary Hospital in Missan, Iraq, [2]Departments of Surgery and Obstetrics, College of Veterinary Medicine, University of Baghdad, Iraq,[3]Departments of Anatomy and Histology, College of Veterinary Medicine, University of Baghdad, Iraq

ABSTRACT

The present study was conducted to evaluate the effect of scaffold fabricated from Nano crab shell and Al-kharit (Papyrus Vaccine) for enhancing the healing of the experimentally induced bone defect in dogs. For this purpose, twenty healthy adult mongrel dogs were used in this study which divided randomly into two equal groups, under general anesthesia, 1 cm bone gap was created in the distal part of the tibia, that fixed by bone plate and screws. Nano crab shell scaffold was implanted. All experimental animals showed normal situation without any infection at the site of operation, while the radiography showed a periosteal and endosteal reaction. Moreover, the gaps were bridged faster in the treated group as compared with the control group. Treated animals showed new bone formation which represented by obvious lamellar bone, haversian canal and osteocyte cells in 90 days. In conclusion, the Nano crab shell scaffold gave better acceleration in the bone healing process, also this scaffolds may provide insight into the clinical repair of large bone defects.

Keywords: Crab shell, Al-kharit, 3D porous scaffold, Dogs, Tissue Engineering

Introduction

Large bone defects resulting from trauma, tumors, osteitis, delayed unions, non-unions, ostoectomies, arthrodesis, and multi fragmentary fractures are a current challenge for surgeons and investigators (1). The main components of the skeletal system are bones and connective tissue; they are composed of cells and an extracellular matrix. The bone graft is considered as a transplanted tissue used in medical procedures when there are neoplasm, diseases, trauma or deformity to replace the broken bone (2). The tissue engineering and regenerative medicine introducing a motivation behind bone development and creation of biological substitutes (scaffolds). While, the scaffold is the primary component of the bone tissue engineering design, for optimal replacement of damaged bone (3). Nano-technology science introduced currently a procedure for the damaged bone, degenerative diseases, congenital deformities, and tumor resection of bone tissue, in addition, to replace the bone by autografts, allografts or xenografts (4).

Nowadays researches are focuses on new materials that have to some extend similar properties to natural bone structures used for bone tissue regeneration. Therefore, bone tissue engineering approach is representing as an alternative treatment for bone repair and losses resulting from injury or disease in order to restore and improve the function of bone tissue (5). One of these materials is natural coral calcium carbonate ($CaCO_3$). It is used as a bone graft substitutes and used for their excellent biocompatibility and bioactivity. This is because it has similar composition to that in bones where the mean diameter of coral's pores is more than 100 µm (average 200 µm, 190-230 µm) allowing the fibro vascular and bone tissue in growth and makes direct integration with bone possible. Natural coral can be converted into porous hydroxyapatite (HA), through a hydrothermal exchange reaction (6). The $CaCO_3$ of crab shell skeleton can change to (HA), $Ca_{10}(P0_4)_6(OH)_2$, which is the main mineral of bone

*Correspondence: saadhassan_1972@yahoo.com. Ministry of Agriculture, Veterinary Directorate, Veterinary Hospital in Missan Iraq, Iraq. Received: 16 May 2020, Accepted: 16 June 2020, Published: 28 December 2020.

used to designing a suitable replacement biomaterial and considered as an ideal bone replacement (7, 8). Formerly the HA had been used as a suitable replacement biomaterial in form of a scaffold for bone grafts in different surgical specialties due to its porous structures (6, 9). All researches were mentioned that the biodegradation of $CaCO_3$ is faster than HA, that is related to the fundamental difference between them. Both $CaCO_3$ and HA are known to be osteoconductive, biocompatible and very inert materials as a bone substitutes, and work as a functional scaffolds for bone formation *in vivo* (10, 11). Therefore, the aim of the present study was to evaluate the effect of Nano composite Porous 3D Scaffold for long bone repair in a canine model.

Materials and Methods

The Ethics Committee of the College of Veterinary Medicine, University of Baghdad approved all procedures used in this study in accordance with the ethical standards of animal welfare. Twenty healthy mongrel dogs, ages 2-2.5 years, and weighing 14-20 kg were used. The animals were kept in separate cages given 0.2 mg/kg body weight ivermectin (Ivomec, Holland) 0.4 ml/kg SC on the 1st and 14th day of acclimatization. The animals were divided into two equal group (n=10). Both groups comprised of animals were carried out to 1 cm bone gap which induced in distal part of the tibia and this gab fixed by using bone plate and screws. First Group (positive control group) was left without additives for healing. In Second group (Scaffold group) was treated by Nano crab shell scaffold implanted. Dogs were euthanized at 4th and 12th weeks post-operation.

Nanoparticles Powder Preparation Derived Crab Shell

The crab shell powder illustrated in (Figure 1) according to (**12**). Thus, was briefly washed, rubbing free of dirt and boil for 5 minutes then cooled at room temperature, and the contents of the crabs were removed leaving behind the shells. The shells were washed thoroughly with clean water and then dry at 50°C for 24 hrs. The crabs were grinding using blender until they turn into powder and sieve at (20 µm) after which they will be packed into McCartney bottles and sterilized for one hour in the oven at 105 °C. The dry-sterilized crab's powder was subjected to biochemical test. Approximately 2 gm of samples was weighed in porcelain dish and placed in a muffle furnace. The temperature was increased gradually till reach 300 °C and maintained for one hour to remove all the crab content materials. The temperature is further increased to 600°C and maintained for five hours until a grayish ash has formed, after which samples were taken out and grinding to nano-particle manual by mortar.

Fabrication Scaffolds by a Heating Method

The first step was to dissolve the Gelatin 20g and Alkharit 20 g in hot deionized water for two hours at 70-80 °C using stirring machine. Dextrin (20 g) was dissolved in deionized cold water and added to gelatin, and then alkharit added to the mixture. Crab powder 20 gm was added to this mixture and stir until completely homogenized.

Air bubbles of vaporized water make a path for porosity, pour the mixture into a cylindrical wax mold with different diameters specially designed for this purpose and then leave for 2-3 days to dry at room temperature. After 48 hours the wax and scaffold molds were left to dry at the same temperature for another two days. Pore with size (30 µm-400 µm) was required for bone ingrowth into porous implants (Figure 1).

Scaffold Characterization

Examination of prepared scaffolds was done by Scanning Electron Microscopy (SEM), (Tuscan Vega 3rd Generation-England) according to (**13**) methods. Cutting of the scaffolds into smaller circular and longitudinal sections were done and sent to the Electron Microscopy Unit, Centre of nano-technology and advance materials, University of Technology for SEM analysis (Tuscan Vega 3rd Generation-England), for SEM analysis. Micro-structural characterization and average pore diameter of measurement based on 300 measurements that were taken from six replicates.

All the surgical processes were conducted under sterile conditions showed in (Figure 2). The dogs were general anesthetized as described by (**14**).

A longitudinal skin incision (8-10 cm) was made at the craniomedial aspect of the tibia. Then the tibialiscranialis and the lateral deep digital flexor muscles were separated by blunt dissection to expose the tibial bone. After that 1 cm of the all thickness of the tibial bone was resected by hand saw. In control group, defect was immobilized by bone plate and screws only. In the treated group, the bone defect was substituted by Nano scaffold and

fixed by bone plate and screws. The muscles, fascia, and skin were closed routinely.

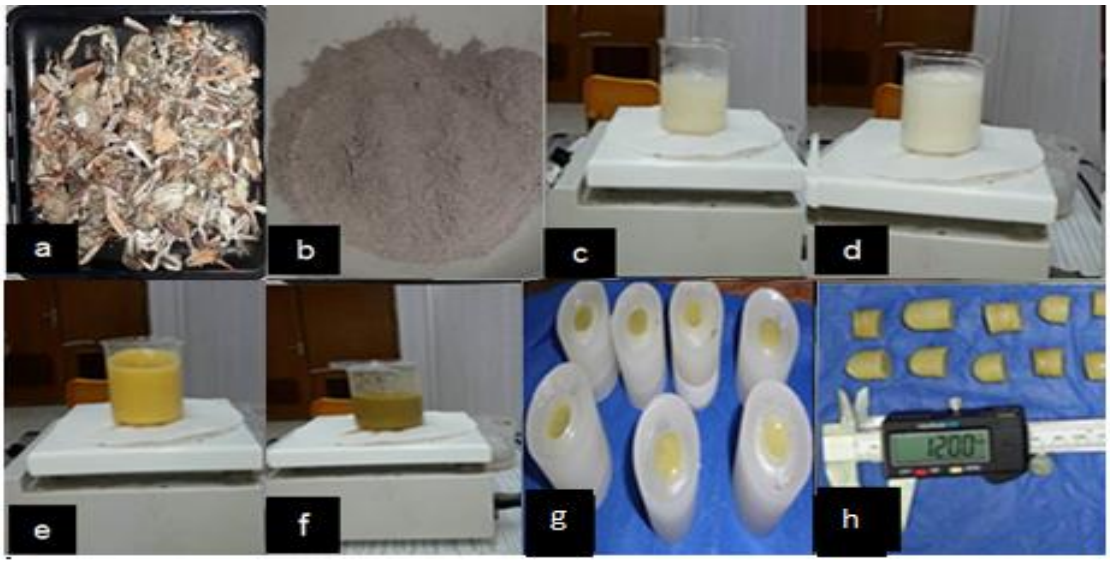

Figure 1. Photograph for preparing scaffold (A) Removed soft tissues. (B) Burn at 600°C. (C) Dissolve gelatinin hot-deionized water. (D) Dissolve dextrin and in cold water and added to gelatin. (E) Al-kharitadded tothe mixture. (F) Crab powderaddedto the mixture. (g) Pour the mixture into a cylindrical wax mold. (h) After removed of wax,measurement and cutting of scaffolds to 1-1.2 cm

Histopathological Examination

Bone specimens were obtained at 4th and 12th weeks post-operatively from both groups. The specimens were fixed in 10% neutral buffer formalin (NBF) for 48 hrs, after that decalcified using 10% formic acid solution for two weeks.

After several chemical processes, the samples sectioned into 5 µm with a microtome (Leica Microsystems, Germany), and finally stained with Hematoxylin and Eosin and Masson's trichrome for view under the light microscope (Olympus, Tokyo, Japan), to evaluate the healing and bone formation at the site of defect.

Figure 2. Photographs of the surgical procedure of creating a defect in tibial bone (black arrow) and scaffold implantation into the defect area in a canine model.The defect is well replaced with sterilized 3D scaffolds (blue arrow) and immobilized by bone plate and screws

Results and Discussion

Scanning Electron Microscopy image for sample of the $CaCO_3$ nanoparticle is shown in Figure 3A. The Figure explains the size particles of the $CaCO_3$ used which distribution in the new product with different sizes. The structure of these products as in similar structure to compact bone, which is an evidence of

the similarity in structure and properties for this composite system as compared with the natural bone. Nano- products contained different pores size around 50 nm-375 nm with homogeneous interior composite. This geometry intra-scaffold new architecture has a major impact on the formation of new bone. The porous scaffolds were created during the process of preparation of scaffolds (Figure 3B).

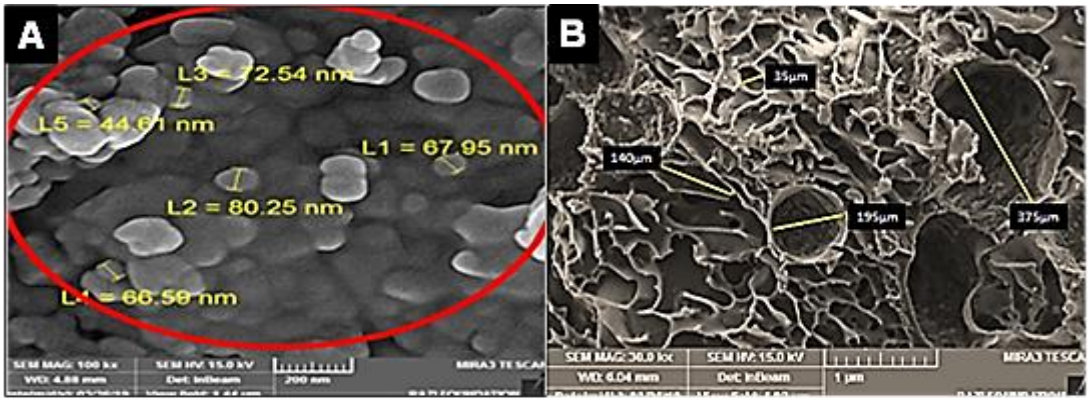

Figure 3. SEM microphotographs of Nano scaffolds prepared by heated method the magnification bars correspond to 1 µm (A) show the particles of Crab shell after ground contains principle material as $CaCO_3$ (B) show porous structure with pore sizes ranging from 30 to 400 µm

It also has been observed that the production of new porous scaffolds is similar to the porous scaffold previously study of advanced manufacturing, with minor differences in porosity and interconnection network. The present study aimed to evaluate the gelatin, dextrin, and Al-kharit ($CaCO_3$) nanoparticle, as scaffold materials for bone tissue restoring applications, in addition to improving nanoparticles usage and coated framework in scaffold design. Dextran was selected for this work for the reason of its known resistance to both protein adsorption and cell adhesion. The quantity of dextran used in scaffold is a determinant of its porosity and interco-nnectivity (**15**). In the present study, the SEM investigation of the developed scaffolds revealed micro-pores with multiple sizes. The physical structure of this micro-porosity of the scaffolds was mainly attributed to air cavities. These supplied spaces to accommodate the effect of swelling on the scaffolds. This observation was similar to those of (**16**, **17**). The radiological sings on control group at 4th week post operation, there was slight periosteal reaction with low opacity at both segments of the tibial defect was observed and no bridging (Figure 4A), while on 12th week post operation, tibial - fibula synostosis and the ends of the bone defect was sclerosed, in addition, rounded ends of the tibial defect and closed medullary cavity revealed nonunion (Figure 4C). In treated group at 4th week post operation, more opacity was observed with periosteal reaction and deposition of osteiod bone and traces of callus as a bridging between both segments of tibial defect (Figure 4B), at 12th week post operation, the density of defect is similar to surroundings cortical part of bone with remodeling and the bone has been taken semi normal shape (Figure 4D). In this study the radiological observations of treated group showed good incorporation between the bone defect ends and the nano crab shell scaffold implant, which allowed good bone formation to occur, mainly from the periphery to the center. After four to twelve weeks post-operation new bone formation was visible at the periphery and covering the entire surface of the nano crab shell scaffold implant at 12th week PO, this may be attributed to the osteoconductive properties of the Nano crab shell scaffold implant so that osteoprogenitor cells can adhere and migrate on the scaffolds, differentiate and finally form new bone, these results agreed with the results of other studies explained that the new bone formation could be a result of osteogenic action of the bone marrow from the defect ends (**18**, **19**). After 12th week PO, the new bone formation covered the entire surface of the nano crab shell scaffold implant without complete degradation of the implant at this period, this may be related to the dense Nano crab shell scaffold implant and large segmental bone defect which needs a long follow up to get complete degradation to be replaced by normal bone, these results came in accordance with the results of study by (**20**) who reported the difficulty to incorporate both osteoconductivey and sufficient mechanical strength into a single implant design because the osteoconduction and biodegr-adation is typically maximized by maximizing porosity, whereas

mechanical properties are frequently maximized by minimizing porosity.

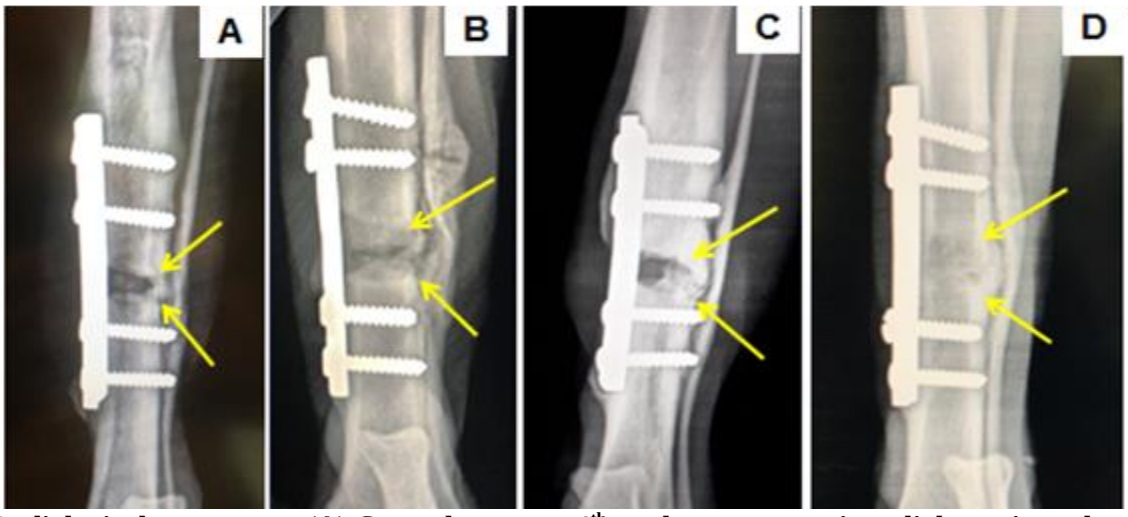

Figure 4. Radiological appearance (A) Control group at 4th weeks post operation, slight periosteal reaction with low opacity at the edge of the defect (C) Control group at 12th week post operation, rounded of bone defect sclerosis of the bone defect edge. (B) Treated group at 4th week post operation, more opacity observed at the site of bone defect with periosteal reaction at the edge of defect and deposition of osteiod bone (D) treated group at 12th week post operation, the density of defect is similar of surroundings cortical part of bone with remodeling and the taken semi normal shape (arrow)

In control group, the histopathological findings after 4th week post-operation showed cellular debris, granulation tissue extended from the site of defect infiltrated by inflammatory cells particularly neutrophils and mononuclear cells in the gap (Figure 5A), and the woven bone lining by osteoblast extended into marrow cavity (Figure 5B).

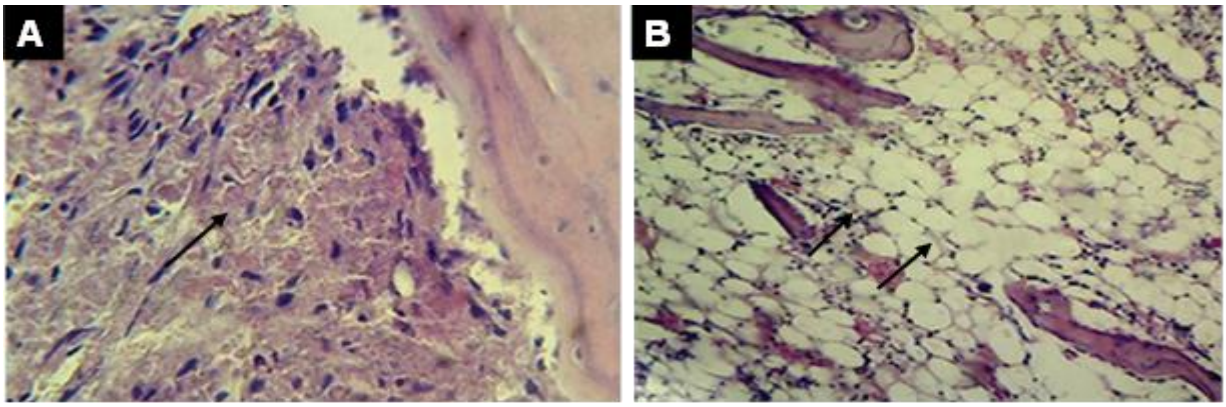

Figure 5. Histopathological section in control group at 4th weeks PO, (A) granulation tissue extended from the site of fracture infiltrated by inflammatory cells particularly mononuclear cells (arrow) (B) bone trabeculae lined by osteoblast extended into narrow cavity (arrow) (H and E, 100×)

At 12th week post-operation, thin layer of compact bone at the end of bone defect extended into granulation tissue (Figure 6A), with a new bone connective tissue and cartilaginous formation was observed in the gap (Figure 6B).

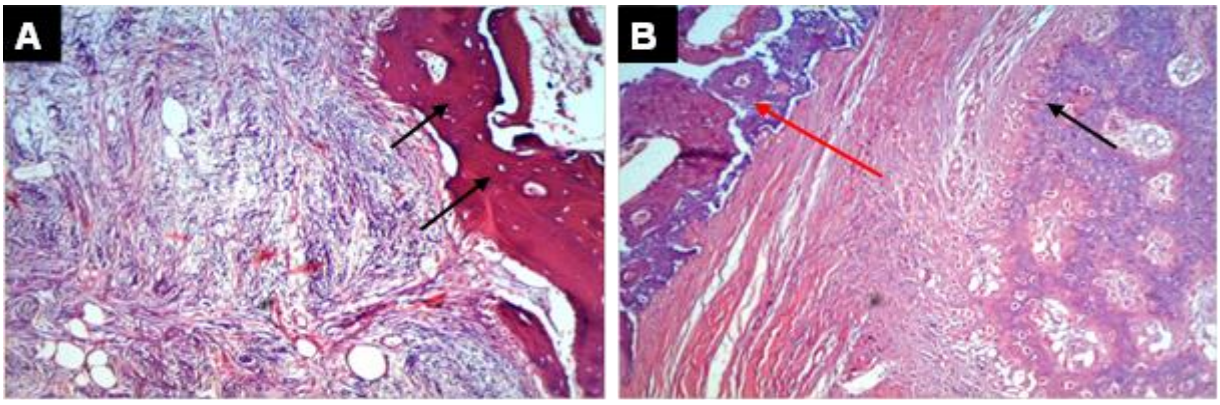

Figure 6. Histopathological section in control group at 12th weeks post-operation, (A) thickness trabecular bone and lamellar bone at the end of defect bone extended into granulation tissue (arrows). (B) a new bone connective tissue (red arrow) and cartilaginous formation(black arrow) (H and E, 100×)

In the treated group after 4th week post-operation the histopathological findings showed trabecular bone with small area of compact bone surrounded by numerous variable size spaces (Figure 7, A and B).

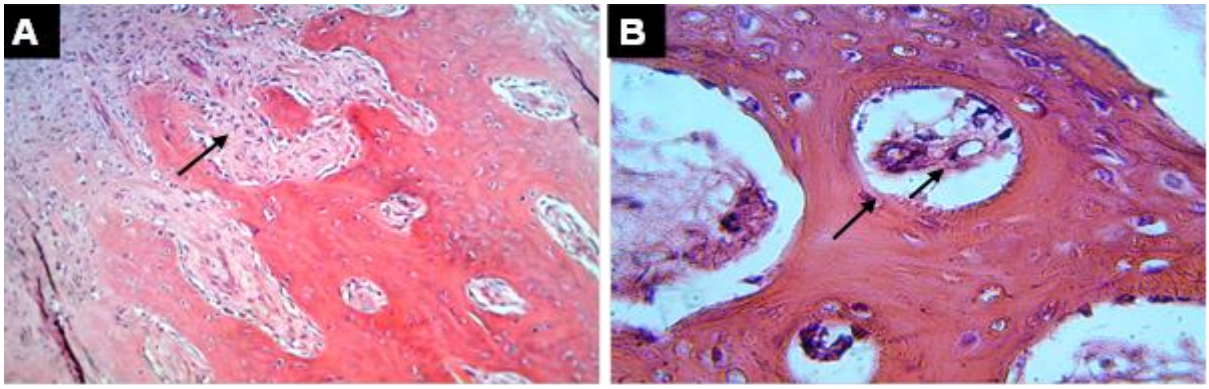

Figure 7. Histopathological section in treated group at 4th weeks post-operation, (A) Compact bone filled the defect bone (black arrow) and contact with old bone (blue arrow) (B) compact bone and active osteoblasts attachment with old one filled the gap (arrow), (H and E, 400×)

At 12th week post operation, showed abundant of compact bone filled the bone gap and connected with the tibia bone (Figure 8, A and B). In special stain of Masson'strichrome showed compact bone and thick layer of trabecular bone (Figure 9, A and B).

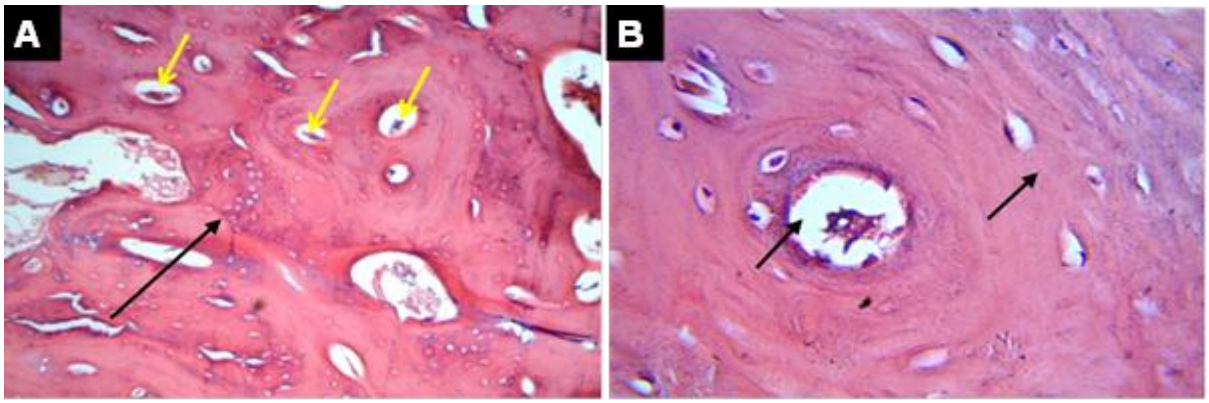

Figure 8. Histopathological section in treated group at 12th weeks post-operation, (A) Thick trabecular bone extended from the site of defect bone (arrow) (B) compact bone attached to the site of defect bone (arrow) (H and E, 400×)

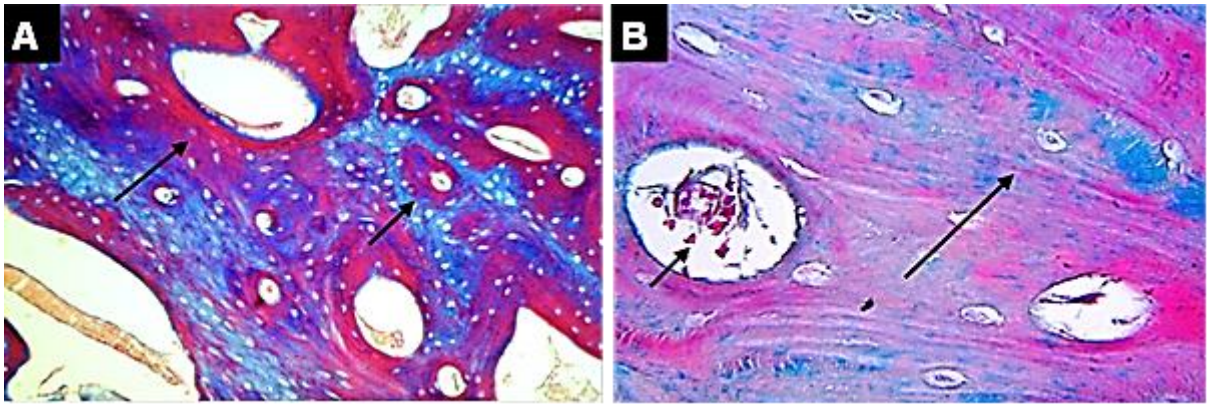

Figure 9. Histopathological section in treated group at 12th weeks post-operation, (A) Trabecular and compact bone tissue (arrow), (B) compact bone (Masson's trichrome, 400×)

In control group reveled granulation tissue formation and the bone defect contained the smallest amounts of new bone from the periphery and patches of cartilage formation. Also (21) showed that newly formed cartilage in the defect accompanied of new bone formation endochonderial ossification and mineralized woven bone. These findings further confirm the positive osteogenic potential of cartilage. Thus, the presence of cartilage in the defect is an important signs of osteogenesis occurring in the soft callus phase (22), in which matrix mineralization of proliferating cartilage changes soft callus into hard callus,and (**23**) demonstrated the presence of fibrous tissue is a sign of poor osteogenic activity. In contrast to newly formed cartilage, when newly formed fibrous tissue accompanies new bone formation no transition exists between the fibrous tissue and newly formed bone. Fibrous tissue is generally not mentioned in the context of bone healing and excessive fibrous tissue formation is known to be a key component in bone non-union. On the other hand, histopathological findings indicated that the defect areas of the experimental animals in both groups showed various amounts of new bone formation, in osteoblast, osteocytes and osteoclast formation and Bone Bridge in treated group compared to control group at intervals of 4th and 12th week PO. This result may be related to the nano crab shell scaffold implant that filled the bone defect and well fitted to the bone cut ends. The nano crab shell scaffold implant acted as an external source of calcium that enhanced the formation of bone tissues. Other worker (24) suggested that an increase in extracellular calcium concentration from an external source possibly acts to down regulate the osteoclastic activity, without disturbing osteoblastic differentiation, leading to a favorable amount of total bone tissue formation. This probably explains the higher amount of bone tissues found within the nano scaffolds groups as initial degrading of the scaffold materials would have observed an influx in the external source of calcium concentration that could have promoted higher osteoblastic activity at an earlier stage. This early stage bone formation possibly explains the presence of higher amount of mineralized bone tissues within the nano crab shell scaffold implant defect site that is indicative of a faster healing property. In addition, the healing process of nano crab shell scaffold implant interface demonstrate sprouting vessels from pre-existent host vessels made a network which probably transports osteoblastic precursor cells into the defect (25). This may related for osteoconductive and probably osteoinductive features of nano crab shell scaffold implant leading to osteogenesis and subsequent remodeling of the newly formed bone (26). Other studies confirmed that the implant pores with a minimum diameter of 50 μm are required for bone ingrowth (27), this result came in line with the results of the present study, while other studies have shown better bone formation when pore size was 300-400 μm (**28**). The larger pores are favorable to vascularization, high oxygenation and subsequent bone formation (29, 8). One important finding from the histopathological examination is regarding the quality of the regenerated tissues. The nano crab shell scaffold implant defect showed a more homogenous form of tissue formation throughout the entire defect compared to the empty defect, which showed signs of healing with minimal formation of regenerated tissue with a higher amount of connective tissues on the upper surface section with underlying distorted tissue and marrow components that similar reported by (30).

This study concluded that using nano-crab shell 3D scaffolds performed excellently in restoring the segment defect in long-term assessment trials. It is noteworthy to mention that there was no toxic or any adverse reactions noticed in all the pre-fabricated materials implanted into the animal model. This study also concluded that 3D scaffolds demonstrated superior qualities in controlling complete growth of new bone alongside the segmental bone defect when assessed by radiological and histological evaluations.

Acknowledgments

The authors would like to thank the College of Veterinary Medicine, University of Baghdad for supporting this study.

References

1. Bigham-Sadegh A, Oryan A. Basic concepts regarding fracture healing and the current options and future directions in managing bone fractures. Int. Wound J. 2015; 12(3): 238-247.
2. Thompson RC,Garg A, Clohisy DR, Cheng EY. Fractures in large-segment allografts. Clin. Orthop. Relat. Res.2000; 270: 227-235.
3. Khan SN, Tomin E, Lane JM. Clinical applications of bone graft substitutes. Orthop. Clin. North Am. 2000; 31:389–98.
4. Yoshikawa T, Nakajima H, Yamada E, Akahane M, Dohi Y, Ohgushi H, et al. In Vivo Osteogenic Capability of Cultured Allogeneic Bone in Porous Hydroxyapatite: Immunosuppressive and Osteogenic Potential of FK506 In Vivo. J. Bone Miner Res.2000; 15:1147-1157.
5. HuangY, Onyeri S,SieweM, Moshfeghian A, Madihally S. *In vitro* characterization of chitosan-gelatin scaffold for tissue engine-ering. Biomaterials.2005; 26:7616-7627.
6. Joschek S, Nies B, Krotz R, Gopferich A. Chemical and physiochemical characterize-ation of porous hydroxyapatite ceramic made of natural bone. Bioma-terials.2000; 21: 1645-1658.
7. Kang HG, Kim SY,Lee YM. Novel Porous Gelatin Scaffolds by Overrun/Particle Leaching Process for Tissue Engineering Applications. J. Biomed. Mater. Res. Part B: Applied Biomaterials. 2006; 79:388–397.
8. Ibrahim SM, Mahmood SK, Razak IS, Yusof LM, Mahmood Z K, Gimba FI, et al. Characterization and In Vitro evaluation of a novel coated nanocomposite porous 3D scaffold for bone repair. Iraqi J. Vet. Sci. 2019; 33(1): 157-173.
9. Lei Y, Rai B, Ho KH, Teoh SH. In vitro degradation of novel bioactive polycapro-lactone-20% tricalcium phosphate composite scaffolds for bone engineering. Mate. Sci. Eng. 2007; 27(2): 293- 298
10. Bong-Soon C, Choon-Ki, L, Kug-Sun H, Hyuk-Joon Y, Hyun- Seung R, Sung-Soo C, et al.Osteoconduction at porous hydroxyl-apatite with various pore conFigureurations. Biomaterials.2000; 21: 1291-1298.
11. Dong J,Kojima H, Uemura T, Kikuchi M, Tateishi T, Tanaka J. *In vivo* evaluation of a novel porous hydroxyapatite to sustain osteogenesis of transplant bone marrow-derived osteoblastic cells. J. Biomed. Mater. Res. 2001; 57(2):208-216.
12. Al-Hussany BFH. Fabrication of cockle shell-Based 3D scaffolds for bone repair. [Dissertation]; Malaysia :University Putra ;2010.
13. Hannink G, Arts J C. Bioresorbability, porosity and mechanical strength of bone substitutes: what is optimal for bone regeneration. Injury.2011; 42(2011): S22-S25.
14. Al-Asadi RN and Al-Marashdi HH.The use of ketamine-xylazine combination as a general anesthesia for dogs. Iraqi J. Vet. Sci. 1990;1(2): 72-81.
15. Kim HW, Kim HE, Salih V. Stimulation of osteoblast responses to biomimetic nanoco-mposites of gelatin–hydroxyapatite for tissue engineering scaffolds. Biomaterials, 2005; 26(25): 5221-5230.
16. Rungsiyanont S, Dhanesuan N, Swasdison S, Kasugai S. Evaluation of biomimetic scaffold of gelatin–hydroxyapatite crosslink as a novel scaffold for tissue engineering: Biocompat-ibility evaluation with human PDL fibroblasts, human mesenchymal stromal cells, and primary bone cells. J. Biomater. Appl.2012; 27(1): 47-54.
17. Przekora A,Ginalska G. Biological properties of novel chitosan-based composites for medical application as bone substitute. Cent. Eur. J. Biol. 2014; 9(6): 634-641.
18. Kang NW, Kim HT, Kang JH, Lee JS, Ahn TY, Jun ES, et al. New Bone Formation Following Transplantation of Stem Cells and

Nanoscale Hydroxyapatite Scaffold Materials into Rabbit Long Bone Defects. J. Korean Orthop. Associ. 2011; 46(1): 18-27.

19. Kim HL, Jung GY, Yoon JH, Han JS, Park YJ, Kim DG,et al. Preparation of nano-sized hydroxyapatite/alginate/chitosan composite scaffolds for bone tissue engineering. Mate. Sci. Eng.2015; 54: 20-25.

20. Lima PAL, Resende CX, de Almeida Soares GD, Anselme K,Almeida LE. Preparation, characterization and biological test of 3D-scaffolds based on chitosan, fibroin and hydroxyapatite for bone tissue engine-ering. Mate. Sci. Eng.2013; 33(6): 3389-3395.

21. Yang L, Tsang KY, Tang HC, Chan HD, Cheah KS. Hypertrophic chondrocytes can become osteoblasts and osteocytes in endochondral bone formation. PNAS.2014; 111(33): 12097-12102.

22. Schell H, Duda GN, Peters AT, Sitsilonis S, Johnson K A,Schmidt-Bleek K. The haema-toma and its role in bone healing. J. Exp. orthop.2017; 4(1): 5-17.

23. Gredes T, Wrobel-Kwiatkowska M, Dominiak M, Gedrange T, Kunert-Keil, C. Osteogenic capacity of transgenic flax scaffolds. Biomed. Tech. 2012; 57(1): 53-58.

24. Pabbruwe MB, Standard OC, Sorrell CC, Howlett CR. Bone formation within alumina tubes: effect of calcium, manganese, and chromium dopants. Biomaterials. 2004; 25(20): 4901-4910.

25. Zhang R, Lee P, Lui VC, Chen Y, Liu X, Lok CN, et al. Silver nanoparticles promote osteogenesis of mesenchymal stem cells and improve bone fracture healing in osteogenesis mechanism mouse model. Nanomedicine: Nanotech. Biol. Med. 2015; 11(8): 1949-1959.

26. Venkatesan J, Pallela R, Bhatnagar I, Kim, SK.Chitosanamylopectin/hydroxyapatite and sulphate/hydroxyapatite composite scaffolds for bone tissue engineering. Int. J. Biol. Macromol. 2012; 51(5): 1033-1042.

27. Jin HH, Kim DH, Kim TW, Shin KK, Jung JS, Park HC, et al. In vivo evaluation of porous hydroxyapatite/chitosan–alginate com-posite scaffolds for bone tissue engine-ering. Int. J. Biol. Macromol. 2012; 51(5): 1079-1085.

28. Mahmood SK, Zakaria MZ, Razak IS, Yusof LM, Mahmood, ZK, Latip MB. In Vivo evaluation of the novel nanocomposite porous 3D scaffold in a rabbit model: hematology and biochemistry analysis. Iraqi J. Vet. Sci. 2018; 32(2): 219-230.

29. Sajesh KM, Jayakumar R, Nair SV,Chennazhi KP. Biocompatible conducting chitosan/ polypyrrole–alginate composite scaffold for bone tissue engineering. Int. J. Biol. Macromol. 2013; 62: 465-471.

30. Thanoon MG, Eesa MJ, Alkenanny ER. Histopathological evaluation of the platelets rich fibrin and bone marrow on healing of experimental induced distal radial fracture in local dogs. Iraqi J. Vet. Med. 2019; 43(1):11-20.

التأثيرات الشعاعية والنسيجية للسقالة الثلاثية الأبعاد المسامية المركبة النانوية من سرطان البحر والخريط على أصلاح العظام

سعـد حسن زبون[١]، محمد جـــواد عيسى[٢] وبهـاء فخري حسين[٣]

[١]وزارة الزراعة، المستشفى البيطري ميسان، [٢] فرع الجراحة والتوليد، كلية الطب البيطري،جامعة بغداد،[٣]فرع التشريح والانسجة، كلية الطب البيطري، جامعة بغداد

الخلاصة

أجريت هذه الدراسة لتقييم تأثير السقالة المصنعة من قشرة سرطان البحر النانوية والخريط (لقاح نبات البردي) لتسريع شفاءعيب العظم المستحدث تجريبياً في الكلاب. لهذا الغرض تم استخدام عشرين كلباً بالغاً صحياً وقسمت إلى مجموعتين متساويتين. تحت التخدير العام، تم إنشاءعيب عظمي بمسافة 1 سم في الجزء البعيد من الظنبوب، بعدها تم زرع سقالة قشرة سرطان البحر النانوية في المجموعة المعالجة وتم التثبيت بواسطة لوحة عظم ومسامير. إذ أظهرت جميع الحيوانات التجريبية عدم وجود مضاعفات طبيعية في موقع العملية، مع تفاعل سمحاقي داخلي وخارجي. علاوة على ذلك تم سد العيوب بشكل أسرع في المجموعة المعالجة مقارنة بمجموعة السيطرة. أظهرت الحيوانات المعالجة تكوين عظمي جديد يمثله عظم صفائحي واضح، وقناة هافرسو خلايا عظمية في 90 يوماً. كشف التقييم سريرياً أن السقالات الثلاثة بإمكانها تلبية جميع المتطلبات الرئيسية التي يمكن من خلاله اعتبارها بديلاً مثالياً للعظام . أعطيت سقالة قشرة سرطان البحر النانوية تسارعاً أفضل في عملية شفاء العظام، كما قد توفر هذه السقالات نظرة ثاقبة للإصلاح السريري لعيوب العظام الكبيرة.

الكلمات المفتاحية: قشرة سرطان البحر، الخريط، الكلاب، سقالة مسامية ثلاثية الأبعاد، كلاب، هندسة الأنسجة.